

Creep deformation and rupture behavior of a laminated metal matrix composite

S. B. BINER

Ames Laboratory, Iowa State University, Ames, IA 50011, USA

E-mail: sbbiner@iastate.edu

In this study, the creep behavior of a laminated composite, composed of layers of metal matrix composite having 20 vol% particulate SiC and 2014-aluminum matrix and 6061-aluminum as the ductile layers, was investigated at 250°C under constant loading. In spite of the absence of delamination between the layers, the observed creep rates of the laminated composite were much higher and rupture times were much shorter than those seen for its constituent layers. This behavior is explained with a model based on laminate theory. © 2002 Kluwer Academic Publishers

1. Introduction

Composites are under development to meet the requirements of advanced structural applications that will operate at elevated temperatures. To achieve these objectives different avenues are being explored, including efforts to increase the fracture toughness of normally brittle ceramics, intermetallics and metal matrix composites by the addition of ductile particles, whiskers or layers. The mechanism of toughening at room temperature due to the presence of ductile reinforcements is now well understood [1–9]; however, there are very limited data available for their high temperature behavior.

In this study, the creep behavior of a laminated composite, composed of layers of metal matrix composite having 20 vol% particulate SiC and 2014-aluminum matrix and 6061-aluminum as the ductile layers, is investigated at 250°C under constant loading. The creep deformation and creep rupture behavior of the laminated composite is compared with those of seen on its constituent layers.

2. Experimental procedures and results

The laminated composite, having 20 vol% SiC particulate reinforced 2014-aluminum matrix composite as the hard layers and 6061-aluminum alloy as the ductile layers with stacking sequence as shown in Fig. 1, was produced by roll bonding. The metal matrix composite was produced by powder metallurgy routes by DWA Inc and received as plate having thickness of about 3.2 mm. The initial thickness of the commercial grade 6061-aluminum alloy was 6.3 mm. Each layer was polished to 400 grid, then chemically cleaned. Stacks were inserted into a stainless-steel container with wall thickness of 3 mm. The rolling was carried out at 475°C and the billets were reduced to give 1.7 mm thick-laminated composite. After rolling, the stainless-steel container was removed by surface machining. The resulting volume fractions in the laminated composite were 57% metal matrix composite and 43% 6061-aluminum alloy.

The creep tests were carried out at 250°C in air under constant load on samples which were 5.10 mm in width and 25.4 mm in uniform gauge length. The loading direction was parallel to the interfaces of the layers. During the creep tests, the creep deformation was continuously monitored through an LVDT attached to the gauge section of the samples.

The variation of the creep strains at 50 MPa stress level with time is shown in Fig. 2. As can be seen, at the same stress level, there was a large difference in the creep strain rates, and the times required to failure were also significantly different. The variation of the observed minimum creep strain rates at different applied stress levels is shown in Fig. 3. These observed creep rates were correlated in the form of Norton's power law,

$$\dot{\epsilon} = \dot{\epsilon}_0(\sigma)^n \quad (1)$$

where σ is the applied stress, n is the creep exponent and $\dot{\epsilon}_0$ is the temperature dependent reference strain rate, and their values are summarized in Table. I. As can be seen from Fig. 3, at low stress levels the observed minimum creep rates are much lower for the metal matrix composite than for the 6061-aluminum, and the creep rates for the composite become considerably larger at higher stress levels. This strong stress dependency of the composite on creep deformation can also be seen from the resulting creep exponent values ($n = 9.75$ for the metal matrix composite and $n = 2.59$ for the 6061-aluminum). This behavior is associated with grain sliding behavior and the evolution of the threshold stresses in composites as discussed in detail in [10–13]. The creep deformation rates of the laminated composite were larger than those of either of its constituents. The stress dependence of the creep deformation rate of the laminated composite was similar to that seen for the metal-matrix composite, in spite of the presence of about 43% 6061-aluminum layers which exhibited much lower creep exponent values.

TABLE I Constants of the Norton's power law obtained from the minimum creep rates for the 6061-aluminum alloy, 20 vol%-2014-aluminum metal matrix composite and laminate

	$\dot{\epsilon}_0$	n
6061-Al alloy	2.846×10^{-1}	2.59
Metal matrix composite	1.049×10^{-23}	9.75
Laminate	3.296×10^{-21}	8.8

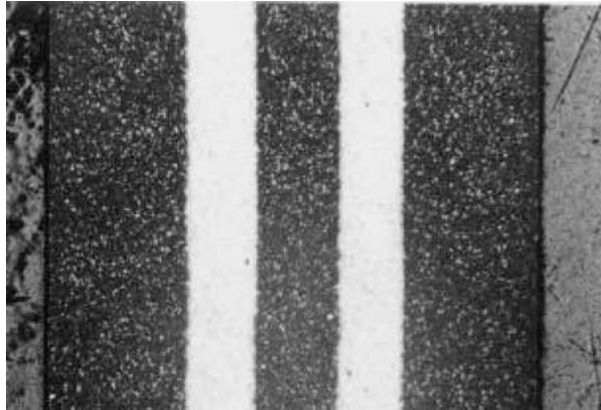


Figure 1 General appearance of the laminated composite, composed of 20 vol% particulate SiC and 2014-aluminum metal matrix composite layers and commercial grade 6061-aluminum alloy layers.

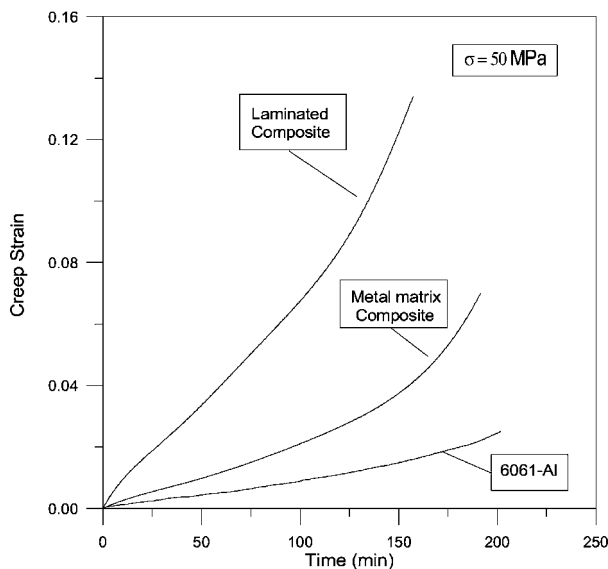


Figure 2 Variation of creep strains with time at 50 MPa stress level in laminated composite, metal matrix composite and 6061-aluminum alloy.

The observed creep rupture times at different stress levels are summarized in Fig. 4. As can be seen from the figure, the rupture times of the metal matrix composite were significantly shorter than the rupture times for 6061-aluminum alloy, particularly at high stress levels. For the laminated composite, the rupture times were again much shorter than those observed for both the metal matrix composite and the 6061-aluminum alloy.

3. Discussion

The evolution of the creep damage in the metal matrix composite is shown in Fig. 5. As can be seen, extensive cavitation occurs at SiC reinforcements; and this behavior is associated with the large grain rotation resulting

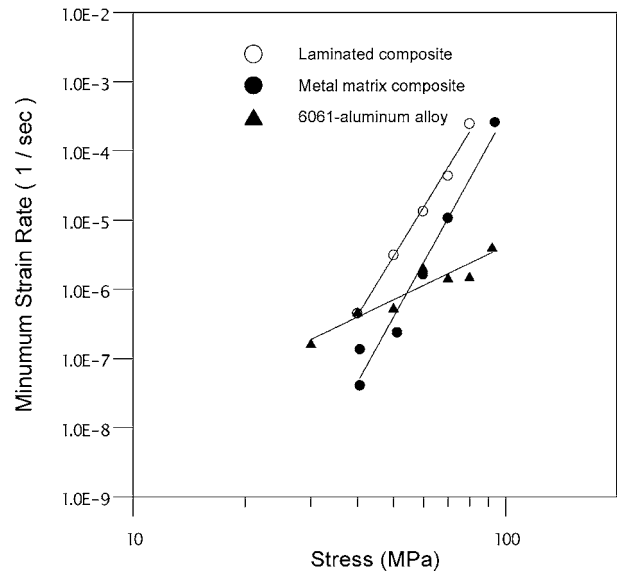


Figure 3 Observed steady-state creep rates at different stress levels for the laminated composite, metal matrix composite and 6061-aluminum alloy.

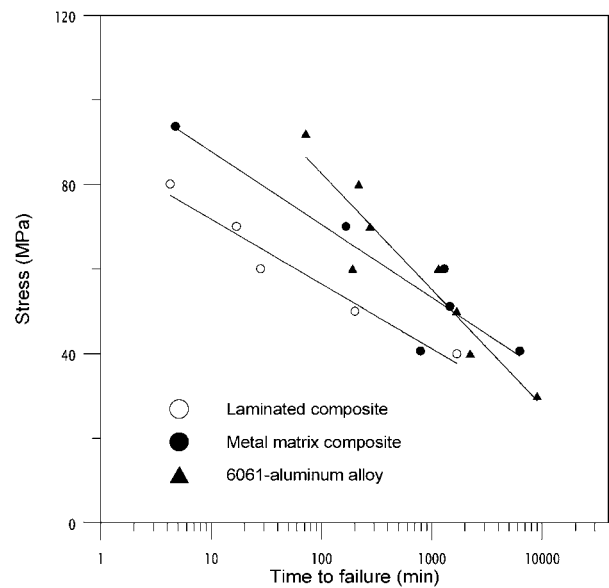


Figure 4 Observed creep rupture times for the laminated composite, metal matrix composite, and for 6061-aluminum alloy.

from grain sliding as described in [10], and also evolution of the threshold stresses as described in [11–13]. The laminated composite exhibited much higher creep deformation rates and much shorter rupture times than those of its constituent layers (Figs 3 and 4). Metallographic and fractographic studies on the fracture surfaces, shown in Fig. 6, did not indicate any delamination between the layers. This observed creep behavior of the laminated composite is associated with the partitioning of the stress between the layers as shown below.

For the laminated composites in the elastic regime under iso-strain condition (i.e., load axis parallel to the interfaces of the layers) the stress levels acting on the layers can be derived as:

$$\epsilon_l = \epsilon_{\text{comp}} = \epsilon_{\text{al}} \quad (2)$$

where, ϵ_l , ϵ_{comp} and ϵ_{al} are the strains in the laminated composite, the metal matrix composite layers, and the

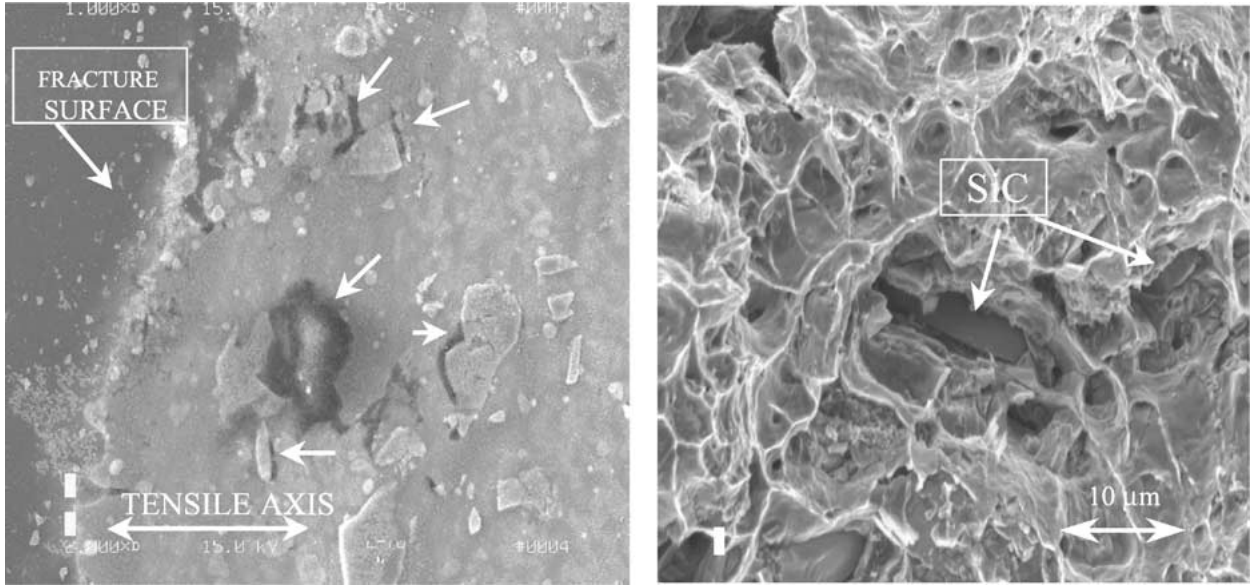


Figure 5 Creep damage evolution behavior in metal matrix composite.

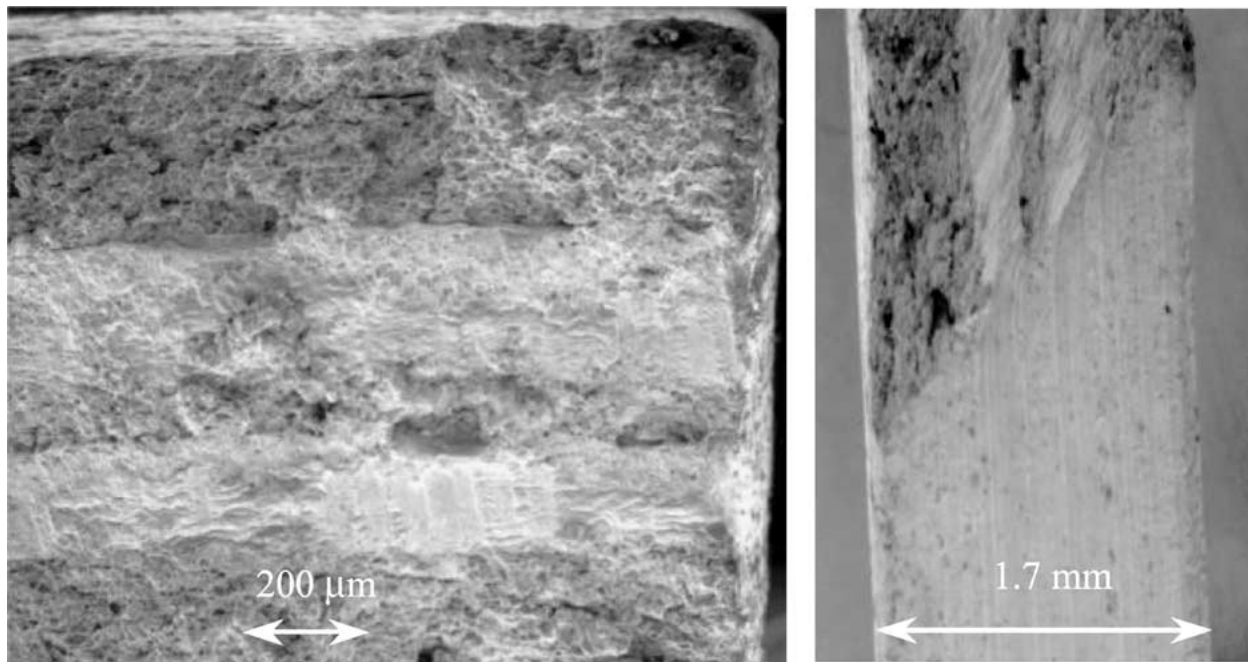


Figure 6 General appearance of the laminated composite after creep rupture at 50 MPa stress level.

6061-aluminum layers respectively. The Young's modulus of the laminated composite E_l can be also estimated from the rule of mixtures as:

$$E_l = V_{\text{comp}} E_{\text{comp}} + V_{\text{al}} E_{\text{al}} \quad (3)$$

where E_{comp} and E_{al} are the Young's modules of the metal matrix composite and the aluminum layers respectively, and V_{comp} and V_{al} are the corresponding volume fractions of the layers in the laminated composite. Using Hooke's law and Equations 2 and 3 the stresses acting on the metal matrix composite layers can be estimated as:

$$\sigma_{\text{comp}} = \frac{\sigma_l}{V_{\text{comp}} + V_{\text{al}} \frac{E_{\text{al}}}{E_{\text{com}}}} \quad (4)$$

The corresponding expression for the aluminum layers is:

$$\sigma_{\text{al}} = \frac{\sigma_l}{V_{\text{al}} + V_{\text{comp}} \frac{E_{\text{comp}}}{E_{\text{al}}}} \quad (5)$$

Inserting the appropriate volume fractions of the layers and Young's modulus values, 110 GPa for the metal matrix composite and 70 GPa for 6061-aluminum alloy in Equations 4 and 5, the stresses acting on the metal matrix composite layers and 6061-aluminum layers were found to be:

$$\sigma_{\text{comp}} = 1.185 \sigma_l \quad \text{and} \quad \sigma_{\text{al}} = 0.754 \sigma_l \quad (6)$$

After establishing the stress portioning among the layers, the creep rate of the composite is assumed to obey:

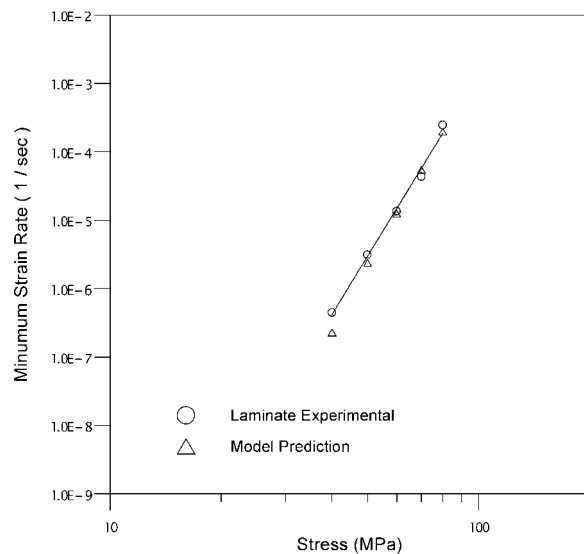


Figure 7 Comparison of predicted and observed creep rates for the laminated composite.

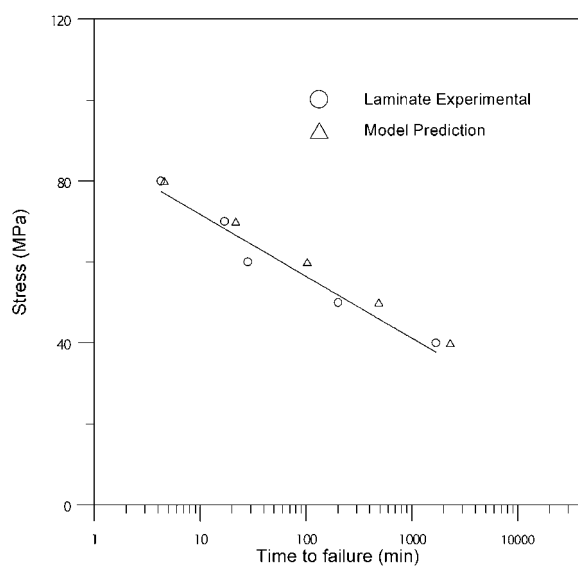


Figure 8 Comparison of predicted and observed creep rupture times for the laminated composite.

$$\dot{\epsilon}_l = (\dot{\epsilon}_0(1.185\sigma)^n)_{\text{comp}} + (\dot{\epsilon}_0(0.754\sigma)^n)_{\text{al}} \quad (7)$$

where the $\dot{\epsilon}_0$ values are the constants and n values are the creep exponents of the Norton's power law for the constituent layers. Equation 7 was written in this form in order to take account of the stress redistribution after the initial elastic deformation. Using this equation, the predicted creep strain rates for the laminate are compared with the measured strain rates in Fig. 7. It can be seen that the predicted values agree with the experimental values. Moreover, by using the same stress portioning values, the predicted and observed rupture times for the laminated composite are compared in Fig. 8, and again the predictions accurately estimate the laminate failure times.

From the above results (Figs 7 and 8), it is clear that the stress portioning among the layers plays a significant role in the creep deformation of the laminated composites. The creep strain rates already higher and creep

rupture time are shorter in the metal matrix composite in comparison to 6061-Al alloy at a given nominal stress level. However, in the laminate, the local stress acting on the metal matrix composite layers is further elevated due to stress portioning, leading to higher strain rates in these layers, and to overall higher strain rates and shorter rupture times for the laminate.

4. Conclusions

In this study, the creep behavior of a laminated composite, composed of layers of metal matrix composite having 20 vol% particulate SiC and 2014-aluminum matrix and 6061-aluminum as the ductile layers, was investigated 250°C under constant loading. The results indicate that:

1. In spite of the absence of delamination between the layers, the observed creep rates and rupture times of the laminated composite were much shorter than those of its constituent phases.
2. Further elevation of the local stress acting on the metal matrix composite layers, due to stress portioning resulting from the large modulus differences of the layers, was shown to be the reason for the creep behavior of this laminate system.

Acknowledgements

This work was performed for the DOE by Iowa State University under contract W-7505-Eng. and also supported by the Director of Energy Research, Office of Basic Sciences. The author thanks L. Reed of Ames Laboratory for his assistance with experimental studies and D. Barnard of Ames Laboratory for carrying out the ultrasound NDE tests during the production of the laminated composites.

References

1. J. T. BEALS and V. C. NARDONE, *J. Mater. Sci.* **29** (1994) 2526.
2. L. SHAW and R. ABBASCHIAN, *Acta Metall. Mater.* **42** (1994) 213.
3. H. C. CAO, B. J. DALGLESIH, H. DAVE, C. ELLIOT, A. G. EVANS, R. MEHRABIAN and G. R. ODETTE, *ibid.* **38** (1990) 2969.
4. V. V. KRSTIC, P. S. NICHOLSON and R. G. HOAGLAND, *J. Amer. Ceram. Soc.* **64** (1981) 499.
5. J. KAJUCH, J. SHORT and J. J. LEWANDOWSKI *Acta Metall. Mater.* **43** (1995) 1955.
6. L. XIAO and R. ABBASCHIAN, *Metall. Trans.* **24A** (1992) 403.
7. T. C. LU, A. G. EVANS, R. J. HECT and R. MEHRABIAN, *Acta Metall. Mater.* **39** (1991) 1853.
8. W. O. SOBOYEJO, F. YE, L-C. CHEN, N. BAHTISHI, D. S. SCHWARTZ and R. J. LEDERICH, *Acta Mater.* **44** (1996) 2027.
9. S. B. BINER, *J. Mater. Sci.* **33** (1998) 3953.
10. *Idem.*, *Acta Mater.* **44** (1996) 1813.
11. *Idem.*, *Ceramic Eng. and Sci. Proceedings* **19** (1998) 475.
12. F. A. MOHAMED, K. T. PARK and E. J. LAVERNIA, *Mat. Sci. Eng. A* **150** (1992) 21.
13. J. CADEK, V. SUSTEK and M. PHATUOVA, *ibid.* **189** (1992) 95.

Received 20 April 2000
and accepted 18 December 2001